The University of Texas ARLINGTON

MATHEMATICS
Preprint Series

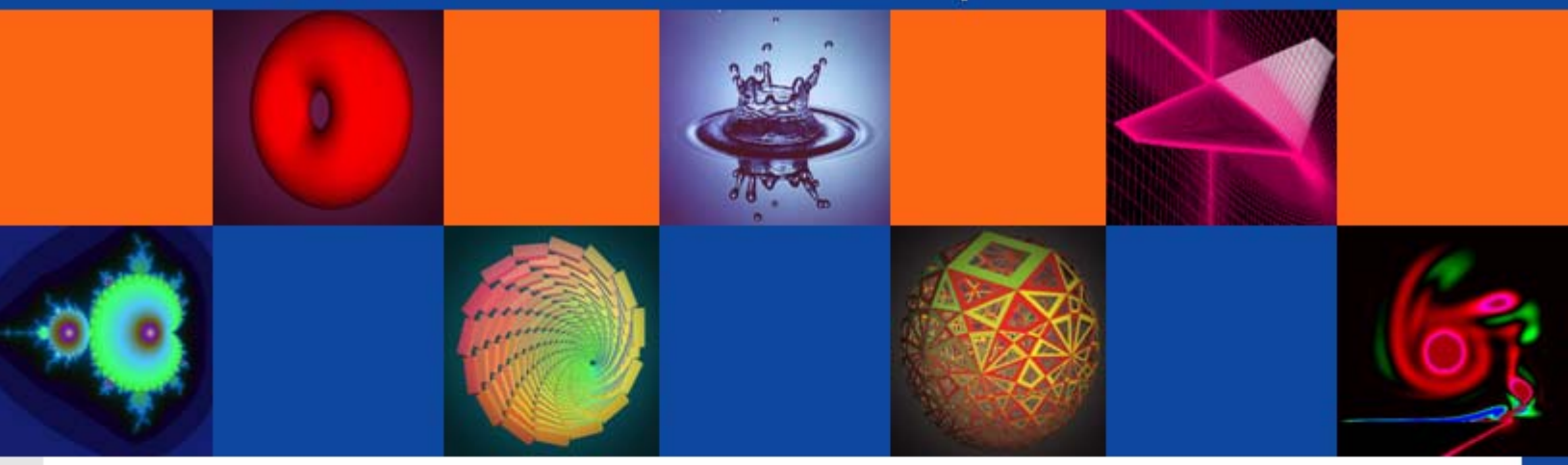

Numerical Simulation Of Multi-Species Biofilms In Porous Media For Different Kinetics

Benito M. Chen-Charpentier
Dobromir T. Dimitrov
Hristo V. Kojouharov

Technical Report 2007-11

http://www.uta.edu/math/preprint/

NUMERICAL SIMULATION OF MULTI-SPECIES BIOFILMS IN POROUS MEDIA FOR DIFFERENT KINETICS

BENITO M. CHEN-CHARPENTIER, DOBROMIR T. DIMITROV, AND HRISTO V. KOJOUHAROV

Abstract. There are bacteria that can form strong biofilms in porous media. These biofilms can be used as biobarriers to restrict the flow of pollutants. For certain contaminants, a second species of bacteria that can actually react with the contaminants can be added to the biobarrier to actually degrade the pollutants. We propose some mathematical models for the formation of these reacting biobarriers under different hypotheses, and numerically solve the resulting equations for the flow, transport and reactions. Qualitative comparisons with some experimental results are also given.

1. Introduction

Biofilm bacteria have been successfully used for forming biobarriers to control the propagation of contaminants in ground water. In [7] we have simulated the growth of biofilms and the formation of biobarriers using nonstandard numerical methods. While subsurface biobarriers substantially control the movement of contaminants, they do not reduce it to zero as is desirable in practice. Recently there have been some experiments [21, 22, 20] where two different types of bacteria are combined to get better results. One type is a strong biofilm-forming bacteria and the other is a bacteria that reacts with the contaminant transforming it into harmless substances. The biofilm-forming bacteria are needed to form the biobarrier so the contaminant transport is reduced and also allows the contaminant-degrading bacteria to establish themselves in the biobarrier and therefore be almost immobile and efficiently destroy the contaminant as it flows by. One of the most common contaminants in ground water is trichloroethene (TCE), which is an unsaturated aliphatic chlorinated hydrocarbon widely used as a decreasing agent. It has been reported that cometabolism is responsible for TCE degradation. Under aerobic conditions microorganisms utilizing a primary substrate, such as methane, phenol or toluene and also ammonia oxidizers, produce enzymes that degrade TCE, [3, 23, 2]. The microbes do not use TCE as a carbon or energy source, but the amount of TCE degraded depends directly on the amount of enzymes produced, which also depends directly on the amount of methane or phenol consumed. According to [22], the toluene ortho-monooxygenase (TOM) pathway is responsible for the degradation of TCE by *B. cepacia* and is located on the TOM plasmid. The authors also calculated the rate of TCE degradation per substrate consumption.

In this paper we model the water flow, the transport of nutrients and a contaminant as well as the growth of biofilm-forming microbes and biodegradation

2000 *Mathematics Subject Classification.* 92D25, 93A30, 65M06, 65M25.

Key words and phrases. multi-species biofilms; reactive solute transport; porous media.

microbes. When we say, for brevity, that a contaminant is used as a nutrient, it should be understood that in the case of TCE, the nutrient is actually methane or phenol or something else, and the amount of TCE degraded is proportional to the amount of that substrate consumed. The paper is organized as follows. In the next section we present the mathematical models. Different models are needed because, depending on the contaminant and nutrient, the reacting bacteria could use either one for growth, or could need both to grow. There is also the question of the effect of thresholds in the amount of nutrients before the bacteria actually feed on them. In Section 3 we show qualitative results of some dual-species biobarrier simulations. The purpose and value of the numerical simulations is to guide future multi-species biofilm experiments that could lead to the design of more effective bioremediation strategies. In the last section we present some conclusions and future research directions.

2. The Mathematical Model

In order to model multi-species biofilm interactions in porous media we consider a three-phase mixture consisting of a liquid phase, a solid rock phase and a biofilm phase. Even though the biofilm can be considered to be part of the solid phase, it is simpler to take it as a separate phase. The six molecular species present in the porous medium are the contaminant, the the contaminant-reducing microbe unable to form a significant biofilm, the strong biofilm-forming bacteria, the nutrient (which can be organic carbon or sometimes oxygen), and the water and rock species. The formulations used in the rest of the paper are valid for diverse species of microbes and chemical substances.

The biofilm forming microbes use the nutrients to grow and to form extra-polymer substances (EPS). The EPS is used to link the microbes together to form the biofilm. One modeling possibility is to consider the EPS an additional species, but this method increases the number of equations and the complexity of the problem. Since the biofilm microbes use a percentage of the available nutrients to form EPS, a second alternative is to consider the microbes and the EPS as one species. The growth parameters for these microbes have to be adjusted accordingly. We will follow the second way and consider that the mass of the biofilm forming microbes includes the EPS.

The fundamental equation for saturated transient ground-water flow of constant density, in horizontal direction, can be written in the form [1]:

$$S_s \frac{\partial h}{\partial t} - \frac{\partial}{\partial x}\left(K \frac{\partial h}{\partial x}\right) = f. \tag{2.1}$$

The single fluid-flow equation (2.1) arises from the mass balance law

$$S_s \frac{\partial h}{\partial t} + \frac{\partial v}{\partial x} = f, \tag{2.2}$$

when we substitute for the specific discharge vector v using Darcy's law

$$v = -K \frac{\partial h}{\partial x}. \tag{2.3}$$

Here $h(x,t)$ denotes the hydraulic head, S_s is the specific storage, K is the saturated hydraulic conductivity, and $f(x,t)$ represent sources or sinks. The specific discharge vector $v(x,t)$, called superficial or Darcy velocity, represents the speed of the water. We assume there are no sources and sinks for the fluid, therefore $f = 0$ in Equation

(2.1). We also assume a piecewise steady-state fluid flow, due to the relatively slow changes in the porous media properties [10]. Also we are modeling very short cores with uniform biofilm distribution so we can take the velocity to be independent of x [10]. Invoking the above simplifying assumptions to Equations (2.1) yields:

$$-\frac{\partial}{\partial x}\left(K\frac{\partial h}{\partial x}\right)=0. \tag{2.4}$$

The transport and reaction of nutrients and contaminants, and the growth of the two microbial species are governed by a system of partial differential equations [1]. We assume that the two types of microbes are immobile, as part of the dual-species biofilm structure. Since the rock phase does not change we assume that the solid rock matrix is stationary and that the diffusion of the two microbial, nutrient and contaminant species in the solid phase is negligible. Therefore we can work only with the liquid and biofilm phases:

$$\begin{aligned}
\frac{\partial}{\partial t}(\phi^{Bio}\rho_B) &= r_B(\rho_B,\rho_K,\rho_C,\rho_T),\\
\frac{\partial}{\partial t}(\phi^{Bio}\rho_K) &= r_K(\rho_B,\rho_K,\rho_C,\rho_T),\\
\frac{\partial}{\partial t}(\phi^{L}\rho_C)+\frac{\partial}{\partial x}(v\rho_C)-\frac{\partial}{\partial x}\left(D\frac{\partial \rho_C}{\partial x}\right) &= r_C(\rho_B,\rho_K,\rho_C,\rho_T),\\
\frac{\partial}{\partial t}(\phi^{L}\rho_T)+\frac{\partial}{\partial x}(v\rho_T)-\frac{\partial}{\partial x}\left(D\frac{\partial \rho_T}{\partial x}\right) &= r_T(\rho_B,\rho_K,\rho_C,\rho_T).
\end{aligned} \tag{2.5}$$

Here ρ_i, $i=B,K,C,T$, represents the intrinsic mass density of the contaminant-degrading microbes, the strong biofilm-forming microbes, the nutrients, and the contaminants , respectively. For a single-fluid flow, the quantity $\phi^L = V_L/(V_L + V_{Bio})$ and the quantity $\phi^{Bio} = V_{Bio}/(V_L + V_{Bio})$, where V_L and V_{Bio} represent the volumes occupied by the liquid and by the biofilm, respectively, are the portions of the void space occupied by the biofilm and the liquid, D is the hydrodynamic dispersion coefficient, and r_i represents the total rate at which species i is produced via reactions and sources.

Let X_B and X_K be the current biodegradation and biobarrier-forming microbial concentrations, respectively, then $\widetilde{X}_B = X_B/\rho_B$ and $\widetilde{X}_K = X_K/\rho_K$ are the corresponding normalized microbial concentrations. We assume that the growth and accumulation of both microbial species in the pore spaces cause changes in the porous media properties. It follows that the changes in porosity and in saturated hydraulic conductivity, for small initial biobarrier-forming microbial concentrations [9], are given by

$$\begin{aligned}
\phi(\widetilde{X}_B,\widetilde{X}_K) &= \phi_0(1-\widetilde{X}_B-\widetilde{X}_K),\\
K(\widetilde{X}_B,\widetilde{X}_K) &= K_0(1-\widetilde{X}_B-\widetilde{X}_K)^{n_k},
\end{aligned} \tag{2.6}$$

respectively, where ϕ_0 is the clean surface porosity, K_0 is the initial hydraulic conductivity and n_k is an experimentally determined parameter which takes values around 3 [9]. For simplicity, from now on we drop the tilde from the normalized microbial concentrations. We assume that the two microbial death rates are proportional to the size of the corresponding microbial populations. Furthermore, direct

interactions in the system are assumed to occur only between the strong biofilm-forming microbial and the nutrients species, and also between the contaminant-degrading microbial and both the nutrients and the contaminants species.

2.1. **Dual-Species Biobarrier Model I.** Incorporating the above simplifying assumptions into Equations (2.5) and using normalized concentrations as the unknowns yields the following governing system of differential equations:

$$\begin{aligned}
\frac{\partial X_B}{\partial t} &= \mu^B\left(S_C, S_T\right) X_B G(X_B + X_K) - k_B X_B \\
\frac{\partial X_K}{\partial t} &= \mu^K(S_C) X_K G(X_B + X_K) - k_K X_K \\
\frac{\partial S_C}{\partial t} + v\frac{\partial S_C}{\partial x} - \frac{\partial}{\partial x}\left(D\frac{\partial S_C}{\partial x}\right) &= -\frac{1}{Y_K}\mu^K(S_C) X_K G(X_B + X_K) \\
&\quad -\frac{F}{Y_B}\mu^B\left(S_C, S_T\right) X_B G(X_B + X_K) \\
\frac{\partial S_T}{\partial t} + v\frac{\partial S_T}{\partial x} - \frac{\partial}{\partial x}\left(D\frac{\partial S_T}{\partial x}\right) &= -\frac{1}{Y_B}\mu^B\left(S_C, S_T\right) X_B G(X_B + X_K)
\end{aligned} \tag{2.7}$$

where μ^j $(j = B, K)$ describes the kinetics of microbial transformations of nutrient and/or contaminant species, Y_B and Y_K are the yield rate coefficients [4], F is the ratio of organic carbon to contaminant consumed, X_K is the normalized concentration of biobarrier-forming microbes, X_B is the normalized concentration of biodegradation microbes, S_C is the concentration of the nutrient, and S_T is the concentration of the contaminant. The coefficients k_B and k_K represent the first-order microbial decay rates and account for the decay processes that diminish the active biomass and for the desorption of the microbes caused by the shear force of the surrounding liquid.

The function G represents the fraction of daughter cell of adherent bacteria that find attachment sites [16]. It is introduced to restrict the growth of microbes as the pores are being plugged and is reasonable to assume that it is a decreasing function, because a more fully saturated wall provides less chance for a daughter cell to find space on it. For example, Freter [14, 15] employs

$$G(X) = \frac{1 - X}{1 - X + \gamma},$$

with γ typically small.

One common assumption in Monod's growth rate for bacteria is that there is only one nutrient that limits the grow [24]. That is, there is an excess of the other nutrients. In this case the rate of substrate utilization has been usually described by [4]:

$$\mu^j(S_i) = \mu^j_{\max}\frac{S_i}{K^j_{S_i} + S_i},$$

$j = B, K$, where S_i is the concentration of the limiting nutrient. For simplification, we assume that the effects of the adsorption process, which is aided by the extracellular polymer substances (EPS), are implicitly incorporated into the growth

rate function through the maximum specific bacterial growth rate $\mu^j_{\max}$. In many cases, the limiting nutrient may change with time and position. In this case the Monod kinetics are given by a product of terms of the above form. This situation is considered in the next subsection. Another scenario is when two or more nutrients have a similar role. For example, they all could be sources of organic carbon. Then the Monod kinetics will be given as the sum of above terms (subsection 2.2). There is also the consideration of thresholds in the concentration values before the bacteria start feeding. The corresponding modifications using cut-off functions to the Monod kinetics are done in subsection 2.1.2 and in case 2 of 2.2. Another way of introducing the thresholds is presented in case 3 of both models.

2.1.1. *Biobarrier Model I - Case 1.* In the first case, the multi-substrate Monod equation [4]:

$$\mu^j(S_1, S_2, \ldots, S_m) = \mu^j_{\max} \prod_{i=1}^{m} \frac{S_i}{K^j_{S_i} + S_i}, \tag{2.8}$$

$j = B, K$, is used to describe the kinetics of microbial transformations of nutrient and contaminant. In System (2.7) the Monod expressions are given by:

$$\begin{aligned} \mu^B\left(S_C, S_T\right) &= \mu^B_{\max} \left(\frac{S_C}{K^B_{S_C} + S_C}\right) \left(\frac{S_T}{K^B_{S_T} + S_T}\right), \\ \mu^K(S_C) &= \frac{\mu^K_{\max} S_C}{K^K_{S_C} + S_C}, \end{aligned} \tag{2.9}$$

where S_i $(i = C, T)$ is the concentration of substrate i, $\mu^j_{\max}$ $(j = B, K)$ is the maximum specific growth rate of microbes j, and $K^j_{S_i}$ is the species S_i half saturation constant [4].

This case corresponds to the pollutant-reducing bacteria needing both substrates (nutrient and pollutant) to grow with no unique limiting one, and the nutrient considered being the limiting one for the biofilm bacteria. There are no thresholds.

2.1.2. *Biobarrier Model I - Case 2.* In the second case, we use a cut-off function to introduce in the model the fact that bacteria need a minimum amount of the nutrients before they start reacting [26]. To account for contaminant degradation ceasing below a certain threshold concentration S_{min}, Reddy and Ford (1996) [25] modified the Monod expression for the growth rate to force $\mu(S)$ to zero when $S - S_{min} < 0$. In the multi-substrate case, the following modified Monod equation [25] is used:

$$\mu^j(S_1, S_2, \ldots, S_m) = \mu^j_{\max} \prod_{i=1}^{m} \frac{1}{2} \frac{S_i}{K^j_{S_i} + S_i} \left[1 + \frac{S_i - S^j_{i,\min}}{\left|S_i - S^j_{i,\min}\right|}\right], \tag{2.10}$$

$j = B, K$, which is used to describe the kinetics of microbial transformations of nutrient and contaminant. Equation (2.10) accounts for the experimental observation that biofilms do not degrade a substrate that is present below a certain "threshold concentration" [5]. Here, $S^j_{i,\min}$ represents the minimum/threshold concentration of substrate i below which the energy that species j gains from the metabolism is less than the energy required to metabolize the substrate i. Rittmann and McCarty [26] presented a theoretical equation for estimating the minimum substrate

concentration needed to support a steady-state biofilm. For a single rate-limiting substrate factor, it was expressed as:

$$S_{\min} = K_S \frac{k}{\mu_{\max} - k}, \tag{2.11}$$

where k, specific bacterial decay rate, $S_{\min}$, minimum substrate concentration, K_S half saturation constant, $\mu_{\max}$ maximum specific bacterial growth rate.

In System (2.7) the following modified Monod expressions are used:

$$\begin{aligned} \mu^B(S_C, S_T) &= \frac{\mu^B_{\max}}{2}\left(\frac{S_C}{K^B_{S_C} + S_C}\left[1 + \frac{S_C - S^B_{C,\min}}{\left|S_C - S^B_{C,\min}\right|}\right]\right)\left(\frac{S_T}{K^B_{S_T} + S_T}\right), \\ \mu^K(S_C) &= \frac{\mu^K_{\max}}{2}\left(\frac{S_C}{K^K_{S_C} + S_C}\left[1 + \frac{S_C - S^K_{C,\min}}{\left|S_C - S^K_{C,\min}\right|}\right]\right), \end{aligned} \tag{2.12}$$

where it is assumed that only the nutrient has a threshold, but that it can be different for each species of bacteria. That is, there must be a minimum amount of nutrient before the bacteria awake and start feeding (See [25]).

2.1.3. *Biobarrier Model I - Case 3.* For comparison purposes, we consider a third case in which the limitations of minimum substrate concentrations are introduced in a different way [28]. These authors suggested the following modified Monod equation:

$$\mu^j(S_1, S_2, \ldots, S_m) = \mu^j_{\max} \prod_{i=1}^{m} \frac{S_i - S^j_{i,\min}}{K^j_{S_i} + S_i - S^j_{i,\min}} \tag{2.13}$$

that is used to describe the kinetics of microbial transformations of nutrient and contaminant. In System (2.7) the following modified Monod expressions are used:

$$\begin{aligned} \mu^B(S_C, S_T) &= \mu^B_{\max}\left(\frac{S_C - S^B_{C,\min}}{K^B_{S_C} + S_C - S^B_{C,\min}}\right)\left(\frac{S_T}{K^B_{S_T} + S_T}\right), \\ \mu^K(S_C) &= \mu^K_{\max}\left(\frac{S_C - S^K_{C,\min}}{K^K_{S_C} + S_C - S^K_{C,\min}}\right), \end{aligned} \tag{2.14}$$

where again it is assumed that only the nutrient has a threshold.

2.2. **Dual-Species Biobarrier Model II.** Here we use the assumption that the nutrients under consideration are all equivalent. That is, they all are carbon sources, or all are oxygen sources, etc. Also, we assume that the other necessary nutrients are in abundant enough quantities that they are never the limiting nutrients, and, therefore are not included in the model. In our case, we assume that the biofilm bacteria needs only the nutrient, and the pollutant-reducing one can use either the nutrient or the pollutant for growth.

Incorporating the above simplifying assumptions into Equations (2.5) and using concentrations as the unknowns yields the following governing system of differential equations:

$$
\begin{aligned}
\frac{\partial X_B}{\partial t} &= \left(\mu^{B,C}(S_C) + \mu^{B,T}(S_T)\right) X_B G(X_B + X_K) - k_B X_B \\
\frac{\partial X_K}{\partial t} &= \mu^K(S_C) X_K G(X_B + X_K) - k_K X_K \\
\frac{\partial S_C}{\partial t} + v\frac{\partial S_C}{\partial x} - \frac{\partial}{\partial x}\left(D\frac{\partial S_C}{\partial x}\right) &= -\frac{1}{Y_K}\mu^K(S_C) X_K G(X_B + X_K) \\
&\quad -\frac{F}{Y_B}\mu^{B,C}(S_C) X_B G(X_B + X_K) \\
\frac{\partial S_T}{\partial t} + v\frac{\partial S_T}{\partial x} - \frac{\partial}{\partial x}\left(D\frac{\partial S_T}{\partial x}\right) &= -\frac{1}{Y_B}\mu^{B,T}(S_T) X_B G(X_B + X_K),
\end{aligned}
\tag{2.15}
$$

where $\mu^{B,i}$ $(i = C, T)$ describes the kinetics of contaminant-reducing microbial of substrate i, and the other scalars/functions are the same as in System (2.7).

Similarly to Section 2.1, we examine the following three cases of microbial kinetics:

- In the first case, we assume that there are no thresholds, so the following single-substrate Monod expressions are used in System (2.15):

$$
\begin{aligned}
\mu^{B,C}(S_C) &= \frac{\mu^{B,C}_{\max} S_C}{K^B_{S_C} + S_C}, \quad \mu^{B,T}(S_T) = \frac{\mu^{B,T}_{\max} S_T}{K^B_{S_T} + S_T}, \\
\mu^K(S_C) &= \frac{\mu^K_{\max} S_C}{K^K_{S_C} + S_C}.
\end{aligned}
\tag{2.16}
$$

- In the second case, similarly to Section 2.1.2, we introduce the thresholds using cut-off functions, and, therefore, the following modified Monod expressions are used in System (2.15):

$$
\begin{aligned}
\mu^{B,C}(S_C) &= \frac{\mu^{B,C}_{\max}}{2}\left(\frac{S_C}{K^B_{S_C} + S_C}\left[1 + \frac{S_C - S^B_{C,\min}}{\left|S_C - S^B_{C,\min}\right|}\right]\right), \\
\mu^{B,T}(S_T) &= \frac{\mu^{B,T}_{\max} S_T}{K^B_{S_T} + S_T} \\
\mu^K(S_C) &= \frac{\mu^K_{\max}}{2}\left(\frac{S_C}{K^K_{S_C} + S_C}\left[1 + \frac{S_C - S^K_{C,\min}}{\left|S_C - S^K_{C,\min}\right|}\right]\right).
\end{aligned}
\tag{2.17}
$$

- In the third case, similarly to Section 2.1.3, we use the alternative model for introducing the thresholds. The following modified Monod expressions

are used in System (2.15):

$$\mu^{B,C}(S_C) = \mu^{B,C}_{\max}\left(\frac{S_C - S^B_{C,\min}}{K^B_{S_C} + S_C - S^B_{C,\min}}\right), \quad \mu^{B,T}(S_T) = \frac{\mu^{B,T}_{\max} S_T}{K^B_{S_T} + S_T}$$
$$\mu^{K}(S_C) = \mu^{K}_{\max}\left(\frac{S_C - S^K_{C,\min}}{K^K_{S_C} + S_C - S^K_{C,\min}}\right). \tag{2.18}$$

3. Simulations

Equations (2.4)-(2.5) represent a coupled system of nonlinear, time-dependent ordinary and partial differential equations that is difficult to solve numerically. A key objective of the numerical simulation is to develop time-stepping procedures that are accurate and computationally stable. We use a sequential solution technique that first solves implicitly for the Darcy velocity v at the current time-level, by solving Equations (2.3) and (2.4). Then the species transport system (2.5) is solved implicitly for the concentrations X_B, X_K, S_C and S_T, in a decoupled fashion [12]. New values of the porosity and the hydraulic conductivity are then calculated using Equation (2.6) and the cycle is repeated by calculating the new velocities.

For the solution of the ordinary differential equation (2.4) we use a standard finite-difference method to calculate h. Then we numerically differentiate using Darcy's law (2.3) to get the velocity field v. The temporal differentiation in the microbial species equations (2.5) uses a forward Euler time integration. The nutrients and contaminants transport equations are solved using a nonstandard finite-difference (NSFD) numerical method [7, 17, 11]. Since we are mainly interested in the steady states of the system, the low-order accuracy of this method is not an issue.

Values of the parameters used in the numerical experiments are summarized in Table 1, below. For comparison purposes of the results and performances of the different models with the three types of reaction kinetics, the values of these parameters in this study were chosen as in [8].

The initial conditions used in the numerical simulations are:

$$S_T(x,0) = 25\ \frac{\mu g}{ml}, \quad X_B(x,0) = X_K(x,0) = \begin{cases} 0.2, & 0.3 \le x \le 0.4 \\ 0, & \text{otherwise} \end{cases} \tag{3.1}$$

and the boundary conditions are:

$$h(0,t) = 0.5\ cm, \quad h(1,t) = 0\ cm,$$
$$S_T(0,t) = 25\ \frac{\mu g}{ml}, \quad \frac{\partial S_T}{\partial x}(1,t) = 0\ \frac{\mu g}{ml \cdot sec}. \tag{3.2}$$

The boundary and initial conditions considered in the biobarrier models are in agreement with Cunningham *et al.,* 1991 [10], most of the reaction parameters are taken from Taylor and Jaffé, 1990 [27], and Fenchel, 1986 [13], and the parameter γ in the function G is taken from Jones and Smith, 2000 [16]. The diffusion that we consider represents the average diffusion in the system, so we are assuming, in our simulations, that the coefficient D is constant.

For ease of calculations, the reactor's length has been scaled to 1 and in all of the figures, presented in this section, the nutrients' and contaminant's concentrations have been scaled by a factor of 1/25 for graphing purposes.

TABLE 1. Parameter values used in the numerical experiments.

Parameters	Values
Initial saturated hydraulic conductivity, K_0	0.2402 cm/sec
Initial porosity, ϕ_0	0.35
Hydrodynamic dispersion coefficient, D	0.0005 cm^2/sec
Parameter, n_k	3
Biofilm microbes decay coefficient, k_K	0.0002 $/sec$
Degrading microbes decay coefficient, k_B	0.0001 $/sec$
Biofilm microbes maximum specific growth rate, $\mu^K_{\max}$	0.0104 $/sec$
Half saturation constant, $K^K_{S_C}$	0.799 $\mu g/ml$
Half saturation constant, $K^B_{S_C}$	0.2199 $\mu g/ml$
Half saturation constant, $K^B_{S_T}$	0.0599 $\mu g/ml$
Threshold substrate concentration, $S^B_{C,\min}$	0.12 $\mu g/ml$
Threshold substrate concentration, $S^K_{C,\min}$	0.07 $\mu g/ml$
Ratio constant, F	0.5 $nut/cont$
Parameter, γ	0.1
Parameters specific to System (2.7)	**Values**
Degrading microbes maximum specific growth rate, $\mu^B_{\max}$	0.00527 $/sec$
Biofilm microbes yield coefficient, Y_K	0.0975 mic_K/nut
Degrading microbes yield coefficient, Y_B	0.04875 $mic_B/cont$
Parameters specific to System (2.15)	**Values**
Degrading microbes maximum specific growth rate, $\mu^{B,C}_{\max}$	0.000439 $/sec$
Degrading microbes maximum specific growth rate, $\mu^{B,T}_{\max}$	0.002635 $/sec$
Biofilm microbes yield coefficient, Y_K	0.078 mic_K/nut
Degrading microbes yield coefficient, Y_B	0.039 $mic_B/cont$

The numerical simulations in the following two subsections, Section 3.2 and Section 3.2, represent different test cases, as extensions of our earlier results [8], and demonstrate the effects of the different cut-offs in the kinetics function.

The different kinetics functions, $\mu(S)$, used in the experiments have the following mathematical properties (See Figure 1). As expected, for large concentrations all three microbial kinetics give the same growth rate. However, differences between the growth-rate curves occur at low substrate concentrations (See Figure 1). Type 2 $(-)$ curve, Equation (2.10), is 0 for values of S below S_{min} and agrees exactly with Type 1 $(--)$ curve, Equation (2.8), for $S > S_{min}$. Type 3 $(.-)$ curve, Equation (2.13), is 0 for $S = S_{min}$, while for values of S greater that S_{min} it has the same profile as Type 1 $(-)$ curve, except that it is horizontally shifted S_{min} units to the right. Unfortunately, for values of S below the threshold S_{min}, Type 3 $(.-)$ curve assumes unrealistic negative values, i.e., has the problem that for small concentrations of the substrate the growth rate is negative (see [28] for justifications of this model).

3.1. **Dual-Species Biobarrier Model I.** The first dual-species biobarrier model (2.7) with standard Monod kinetics (2.9) has been validated in [8] with the porous

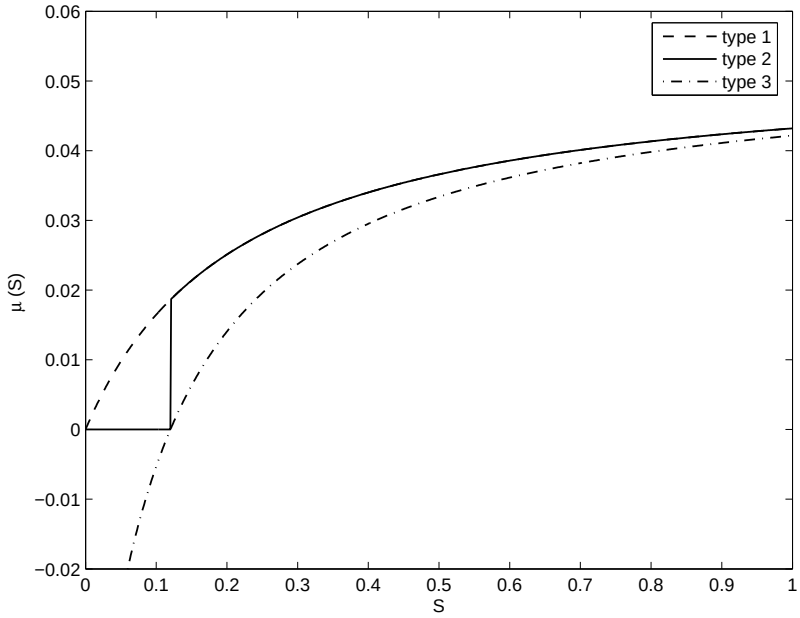

FIGURE 1. Representative plots of the three different types of microbial kinetics (for a single substrate) — Equation (2.8), (2.10), (2.13) — examined in this paper.

media experiments done by Cunningham *et al.,* 1991 [10] for a $5\,cm$-long reactor packed with $0.70\,mm$, in diameter, sands in the absence of biodegradation microbes.

In our first simulation, we consider initial and boundary conditions for S_C that correspond to a high nutrient concentration experiment [21], i.e., $S_C(x,0) = S_C(0,t) = 175\,\mu g/ml$. Numerical experiments are only presented for the standard Monod kinetics (no thresholds), since results are identical as with the first modified Monod kinetics and very similar results with the second modified Monod kinetics. This is clearly the case, since the thresholds are smaller than the steady state values for the nutrient. In this scenario, the steady-state biofilm-forming microbes's population density is about ten times that of the contaminant-degrading microbe's population density (Figure 2, top).

In our second simulation, the initial and the boundary conditions for S_C correspond to a low nutrient concentration experiment [21], i.e., $S_C(x,0) = S_C(0,t) = 17.5\,\mu g/ml$, where the substrate concentration is 10 times smaller than that in the previous simulation. Numerical experiments include all three different Monod kinetics (Figure 2, bottom, and Figure 3. The results are different because for the model with no threshold, the steady state value of the nutrient is now below the threshold used for the other two models. As expected the model with no threshold produces the greater reduction in the amount of pollutant. But, except for the amount of nutrients left, all three models produce similar results. See Figure 4.

Comparing the high nutrient case with the low nutrient one, the results show that the low nutrient one is more efficient in reducing the concentration of the

pollutant. This is because at high concentrations, the biofilm forming bacteria wins the growth race and get much bigger than the pollutant-reducing one. Thus, there is less capacity for eliminating the pollutant. As shown in the next subsection, in Model II the results in terms of contaminant degradation potential at low and high nutrient supply are slightly different.

3.2. **Dual-Species Biobarrier Model II.** In this subsection we simulate the porous media experiments done by Komlos *et al.,* [21, 22, 20] at the Center for Biofilm Engineering, Montana State University. In these experiments the pollutant-reducing bacteria can use either the pollutant or the nutrient as carbon source. This corresponds to our model II. where the Monod growth rate is the same of the separate growth rates. Now the biofilm bacteria has only one carbon source versus two for the other microbes.

In the first (high nutrient supply) experiment the initial and boundary conditions for X_B, X_K and S_T are the same as in the first simulation. The initial and the boundary conditions for S_C correspond to the high substrate concentration case, i.e., $S_C(x,0) = S_C(0,t) = 175\,\mu g/ml$. In this high substrate experiment, as in the corresponding numerical experiment in Section 3.1, the steady-state biofilm microbes population density is almost an order-of-magnitude higher than that of the contaminant-degrading microbe's population density (Figure 5, top, and Figure 7-(a)). But the amount of *B. cepatia* is larger than for model I, and therefore there is an increase in the reduction of the contaminant.

As in Section 3.1, our second simulation corresponds to a low substrate concentration case, i.e., $S_C(x,0) = S_C(0,t) = 17.5\,\mu g/ml$, where S_C is 10 times smaller than that in the first (high nutrient supply) experiment. Numerical experiments include all three different Monod kinetics (Figure 5, bottom, and Figure 6), where simulations show even smaller differences, when compared to the first model, between the different results.

The low substrate experiment shows that the degrading microbes population density is almost an order-of-magnitude higher than the one for the biofilm microbes. This is even though the biofilm microorganism has a growth rate higher than the the degrading microbes (Table 1), but the latter can use either the pollutant or nutrient as its food source. This second numerical experiment confirms what was observed in practice [21, 6], that slower growing organisms are able to persist at high cell concentrations in some low nutrient environments. As can be seen from Figure 7, the biofilm forming bacteria growth is much slower for low substrate concentrations which allows the degrading bacteria to grow more and therefore eliminate more contaminants.

The dual-species simulation results, under conditions of low and high nutrient supply, qualitatively match actual experiment results done by Komlos *et al.,* [21, 22, 20]. The presence of a threshold reduces the amount of contaminant eliminated as expected, but does not change the results significantly. The contaminant degradation potential is larger at low substrate concentrations since the biofilm microbes slower growth allows the other microbes to grow more and therefore degrade more contaminant. This lower substrate concentration produces a more efficient reacting biobarrier. Long-term numerical simulation results of contaminant degradation are in agreement with actual experiments presented in [18].

4. Conclusions and Future Research

The motive for this research was to gain a better understanding of the interactions between two microbial species as part of a single biofilm capable of performing multiple functions (bioremediation, biofilm formation, etc.), and to also numerically compare the differences in results between three of the most widely used, in the biofilm literature, reaction kinetics. We have presented a mathematical model for the flow, the transport of nutrients and contaminants, and the growth of two types of microorganisms in porous media, under different hypotheses. The coupled system of equations was solved numerically in a sequential way using mixed-finite elements for the flow and a nonstandard method for the transport equations. Nonstandard methods work well in conditions where there is transport and nonlinear reactions as in this case. And the coupling of the numerical methods produces a method for a very complicated problem that is stable and fairly accurate.

The colony forming unit (CFU) used in the [21, 18] is only a qualitative measure of population densities, i.e., results of measurements depend on the viability of the cells that have been sampled from the experiments. Since results of the actual measurements change with experimental conditions, in this paper we were able to make only qualitative comments on the behavior of dual-species biofilms. The use of the two types of bacteria looks very promising as shown by the actual experiments [19, 21, 18] and by our numerical simulations. The dual-species biobarrier experiments show that varying the substrate concentration can provide a mechanism to control the fraction of each organism in the dual-species biofilm, and therefore enhance its contaminant degradation potential.

Even though, biologically, the three different kinetics reactions used in the models imply different scenarios, differences between the profiles predicted by the models were negligible. The different kinetics models yielded qualitatively similar results, although there were small quantitative differences. However, our simulations show that in practice the different hypothesis don't seem to show too much of important difference, especially when the models are going to be used for the design of biobarriers.

In real life, the biofilm would spread in the porous medium, which our mathematical model does not allow in its current form. In order to include this in the model, spatial transport terms in the equations for the biomass densities would be needed. Our future work will allow the degrading bacteria some movement, will let biofilm bacteria detach and will consider more spatial dimensions.

References

[1] M.B. Allen, *Basic mechanics of oil reservoir flows*, in Multiphase Flow in Porous Media, M.B. Allen III, G.A. Behie, and J.A. Trangenstein, Lecture Notes in Engineering, vol. 34, pp. 1–81 (C.A. Brebia and S.A. Orszag, Eds.), Springer-Verlag, New York, NY, 1988.

[2] D.J. Arp, C.M. Yeager, M.R. Hyman, *Molecular and cellular fundamentals of aerobic cometabolism of trichloroethene*, Biodegradation **12** 2001, 81–103.

[3] D.M. Bagley, *Systematic approach for modeling tetrachloroethene bio-degradation*, J. Environ. Eng. **124** 1998, 1076–1086.

[4] J.E. Bailey, D.F. Ollis, *Biochemical Engineering Fundamentals*, McGraw-Hill, New York, NY, 1986.

[5] E.J. Bower, P.L. McCarty, *Modeling of trace organics biotransformation in the subsurface*, Ground Water **22** (1984) 433–440.

[6] A.K. Camper, W.J. Jones, J.T. Hayes, *Effect of Growth Conditions and Substratum Composition on the Persistence of Coliforms in Mixed-Population Biofilms*, Appl. Environ. Microbiol., **62** (1996), 4101–4018.

[7] B.M. Chen, H.V. Kojouharov, *Non-standard Numerical Methods Applied to Subsurface Biobarrier Formation Models in Porous Media*, Bull. Math. Biol., **61** (1999), 779-798.

[8] B.M. Chen, H.V. Kojouharov, *Numerical simulation of dual-species biofilms in porous media*, Applied Numerical Mathematics, **47:3-4** (2003) 377–389.

[9] T.P. Clement, B.S. Hooker, R.S. Skeen, *Microscopic Models for the Predicting Changes in the Saturated Porous Media Properties Caused by Microbial Growth*, Ground Water, **34:5** (1996), 934–942.

[10] A.B. Cunningham, W.G. Characklis, F. Abedeen, D. Crawford, *Influence of the Biofilm Accumulation on Porous Media Hydrodynamics*, Environ. Sci. Technol., **25:7** (1991), 1305–1311.

[11] D.T. Dimitrov, H.V. Kojouharov, *Stability-preserving finite-difference methods for general multi-dimensional autonomous dynamical systems*, Int. J. Numer. Anal. Model. **4:2** (2007) 282–292.

[12] R.E. Ewing, T.F. Russell, *Efficient time-stepping methods for miscible displacement problems in porous media*, SIAM J. Numer. Anal., **19** (1982), 1–66.

[13] T. Fenchel, *The Ecology of Heterotrophic Microflagellates*, Advances in Microbial Ecology, vol. 9, pp. 57–97, Plenum Press, New York, NY, 1986.

[14] R. Freter, *Mechanisms that control the microflora in the large intestine*, in Human Intestinal Microflora in Health and Disease, D. Hentges, ed., Academic Press, New York, 1983, pp. 33-54.

[15] R. Freter, H. Brickner, S. Temme, *An understanding of colonization resistance of the mammalian large intestine requires mathematical analysis*, Microecology and Therapy, 16 (1986), pp. 147-155.

[16] D. Jones, H. Smith, *Microbial Competition for nutrient and wall sites in plug flow*, SIAM J. Appl. Math., **60:5** (2000), 1576–1600.

[17] H.V. Kojouharov, B.M. Chen, *Non-Standard Eulerian-Lagrangian Methods for Advection-Diffusion-Reaction Equations*, Applications of the Nonstandard Finite Difference Schemes, pp. 55–108, World Sci. Publishing, River Edge, NJ, 2000.

[18] J. Komlos, *Effect of Co-Substrate Concentration on Dual-Species Population Distribution, Permeability Reduction and Trichloroethylene Biodegradation in Porous Media*, Ph.D. Dissertation in Civil Engineering, Montana State University, September 2001.

[19] J. Komlos, A.B. Cunningham, R.R. Sharp, *Population dynamics in a multi-species biofilm for the creation of a reactive biobarrier*, Proceedings of the 1999 Conference on Hazardous Waste Research, pp. 158–166 (Larry E. Erickson, Ed.), Great Plains/Rocky Mountain HSRC, Manhattan, KS, 2000.

[20] J. Komlos, A.B. Cunningham, A.K. Camper, R.R. Sharp, *Varying substrate concentration to enhance TCE degradation in dual-species bioreactors*, Sixth International In Situ and On Site Bioremediation Symposium, San Diego, CA, USA, 4-7 June 2001, pp. 117-124.

[21] J. Komlos, A.B. Cunningham, A.K. Camper, R.R. Sharp, *Effect of Substrate Concentration on the Dual-Species Population Density of Burkholderia cepatia* $\mathrm{PR1-pTOM_{31c}}$ *and Klebsiella oxytoca in Porous Media*, preprint.

[22] J. Komlos, A.B. Cunningham, A.K. Camper, R.R. Sharp, *Interaction of Klebsiella oxytoca and Burkholderia cepatia in Dual-Species Batch Cultures and Biofilms as a Function of Growth Rate and Substrate Concentration*, Microbial Ecology, Published online: 28 January 2005.

[23] S. Lee, W.M. Moe, K.T. Valsaraj, J.H. Pardue, *Effect of sorption and desorption resistance on aerobic trichloroethene biodegradation in soils*, Environmental Toxicology and Chemistry **21**, (2002) 1609–1617.

[24] J. Monod, *The growth of bacterial cultures*, Annu. Rev. Microbiol., 3, pp. 371-394, 1949.

[25] H.L. Reddy, R.M. Ford, *Analysis of biodegradation and bacterial transport: Comparison of models with kinetic and equilibrium bacterial adsorption*, J. Contaminant Hydrology **22:3-4** (1996) 271–287.

[26] B.E. Rittmann, P.L. McCarty, *Model of steady-state-biofilm kinetics*, Biotechnol. Bioeng. **22** (1980) 2343-2357.

[27] S.W. Taylor, P.R. Jaffé, *Subsurface and Biomass Transport in a Porous Medium*, Water Resources Research, **26** (1990), 2181–2194.
[28] S. Zhu, S. Chen, *An experimental study on nitrification biofilm performances using a series reactor system*, Aquacultural Engineering **20:4** (1999) 245–259.

Benito M. Chen-Charpentier
Department of Mathematics, University of Wyoming, Laramie, WY 82071-3036, USA
E-mail address: bchen@uwyo.edu

Dobromir T. Dimitrov
Department of Ecology and Evolutionary Biology, University of Tennessee at Knoxville, Knoxville, TN 37996-1610, USA
E-mail address: ddimitr1@utk.edu

Hristo V. Kojouharov
Department of Mathematics, University of Texas at Arlington, Arlington, TX 76019-0408, USA
E-mail address: hristo@uta.edu

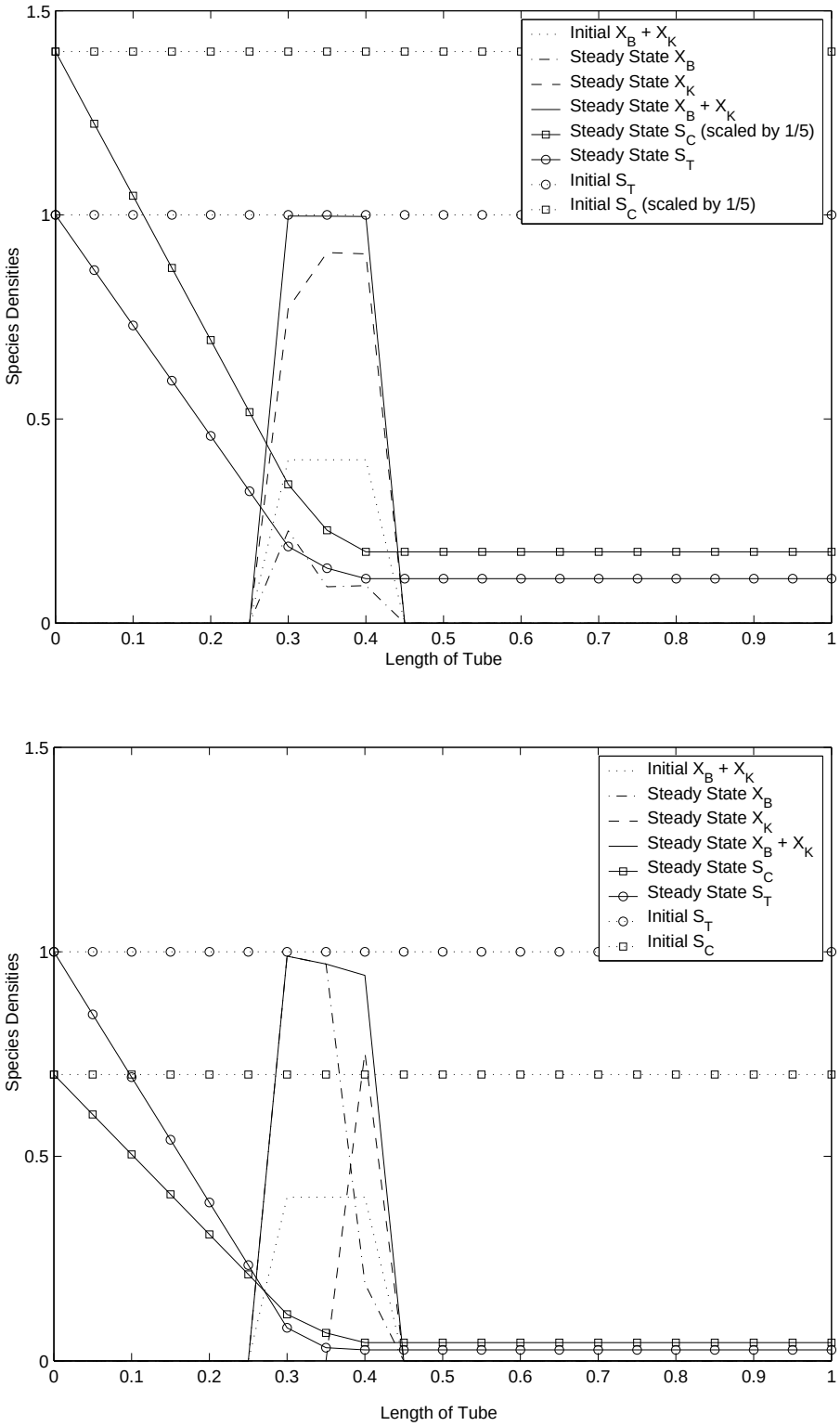

FIGURE 2. Numerical simulation results for the dual-species biobarrier model I, System (2.7), with standard Monod kinetics, Equations (2.9) — at high nutrient (top) and at low nutrient (bottom) supply into the system.

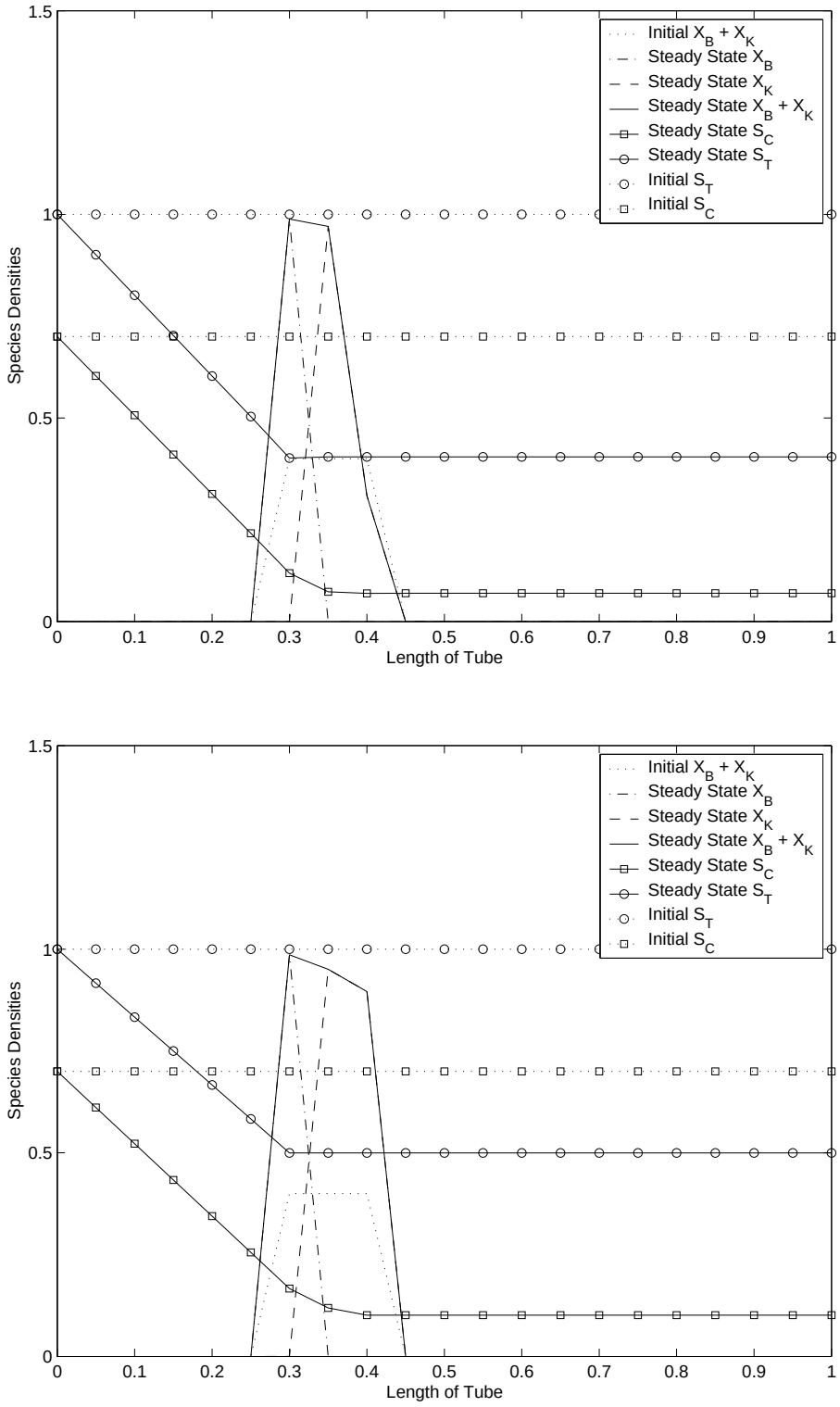

FIGURE 3. Numerical simulation results for the dual-species biobarrier model I, System (2.7), with different modified Monod kinetics, Equations (2.12) (top) and Equations (2.14) (bottom), at low nutrient supply into the system.

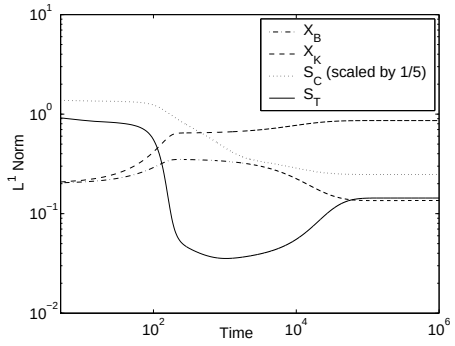

(a) System (2.7) with Equations (2.9)

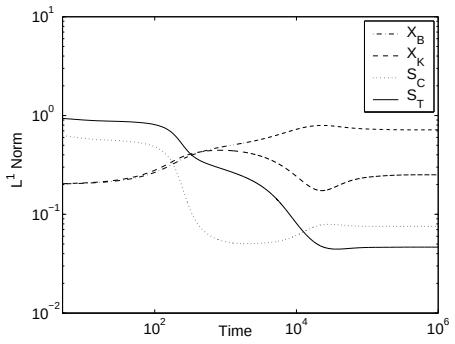

(b) System (2.7) with Equations (2.9)

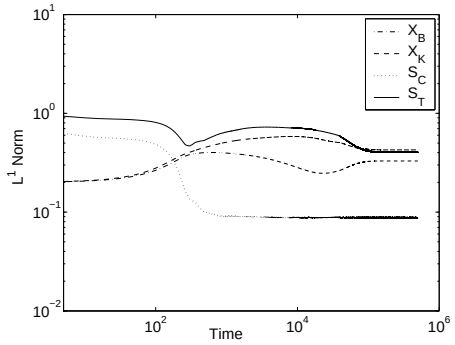

(c) System (2.7) with Equations (2.12)

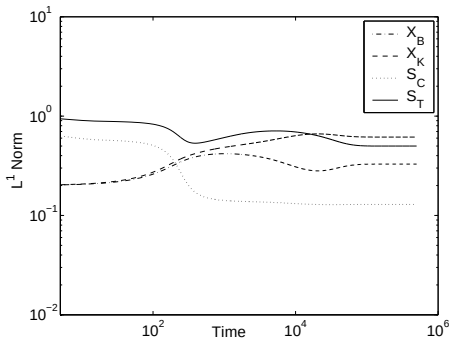

(d) System (2.7) with Equations (2.14)

FIGURE 4. Log-log scale plots of the L^1 norms of X_K, X_B, S_C, and S_T, versus time — at high nutrient (a) and at low nutrient (b), (c), and (d) supply into the system for the dual-species biobarrier model I with different Monod kinetics.

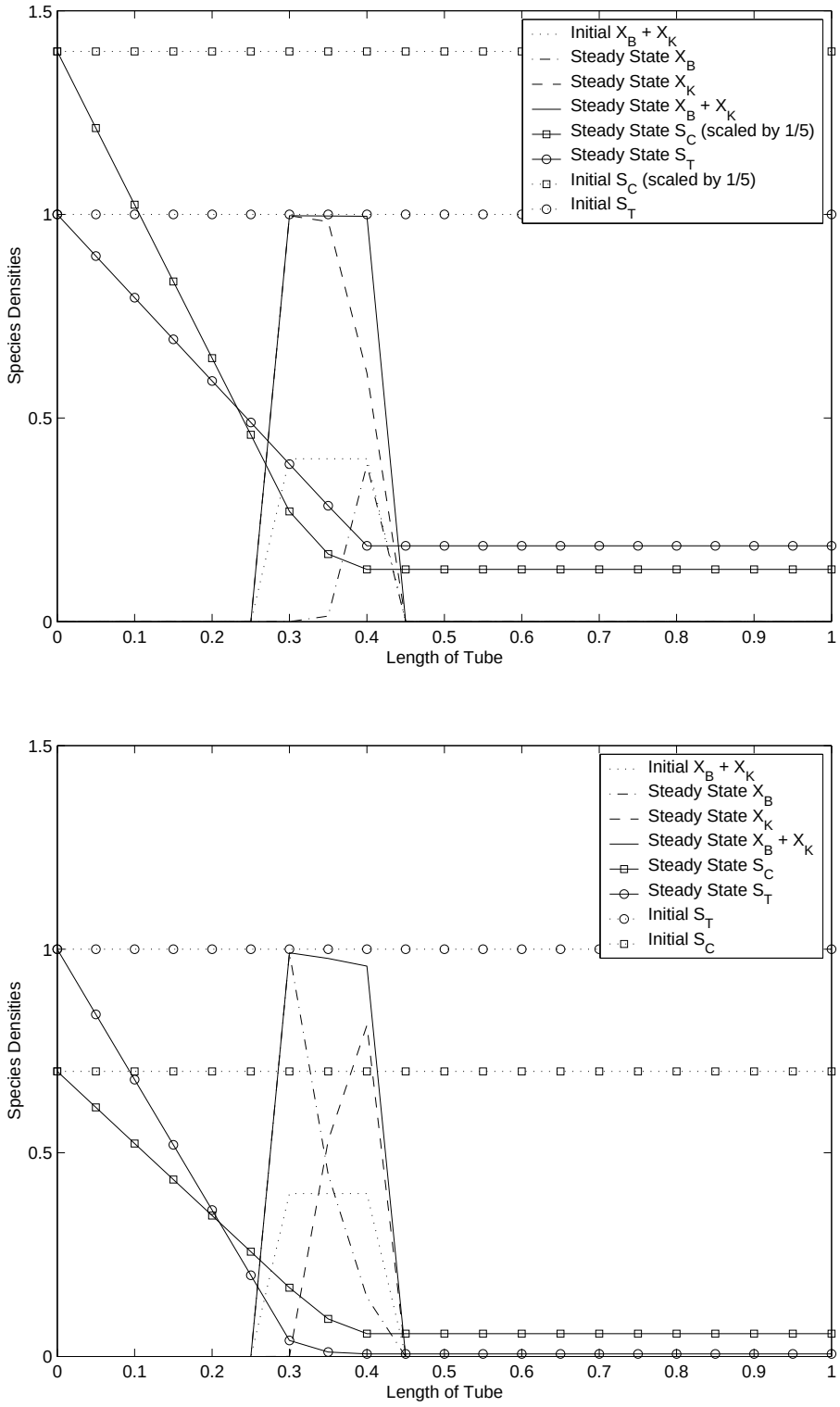

FIGURE 5. Numerical simulation results for the dual-species bio-barrier model II, System (2.15), with standard Monod kinetics, Equations (2.16) — at high nutrient (top) and at low nutrient (bottom) supply into the system.

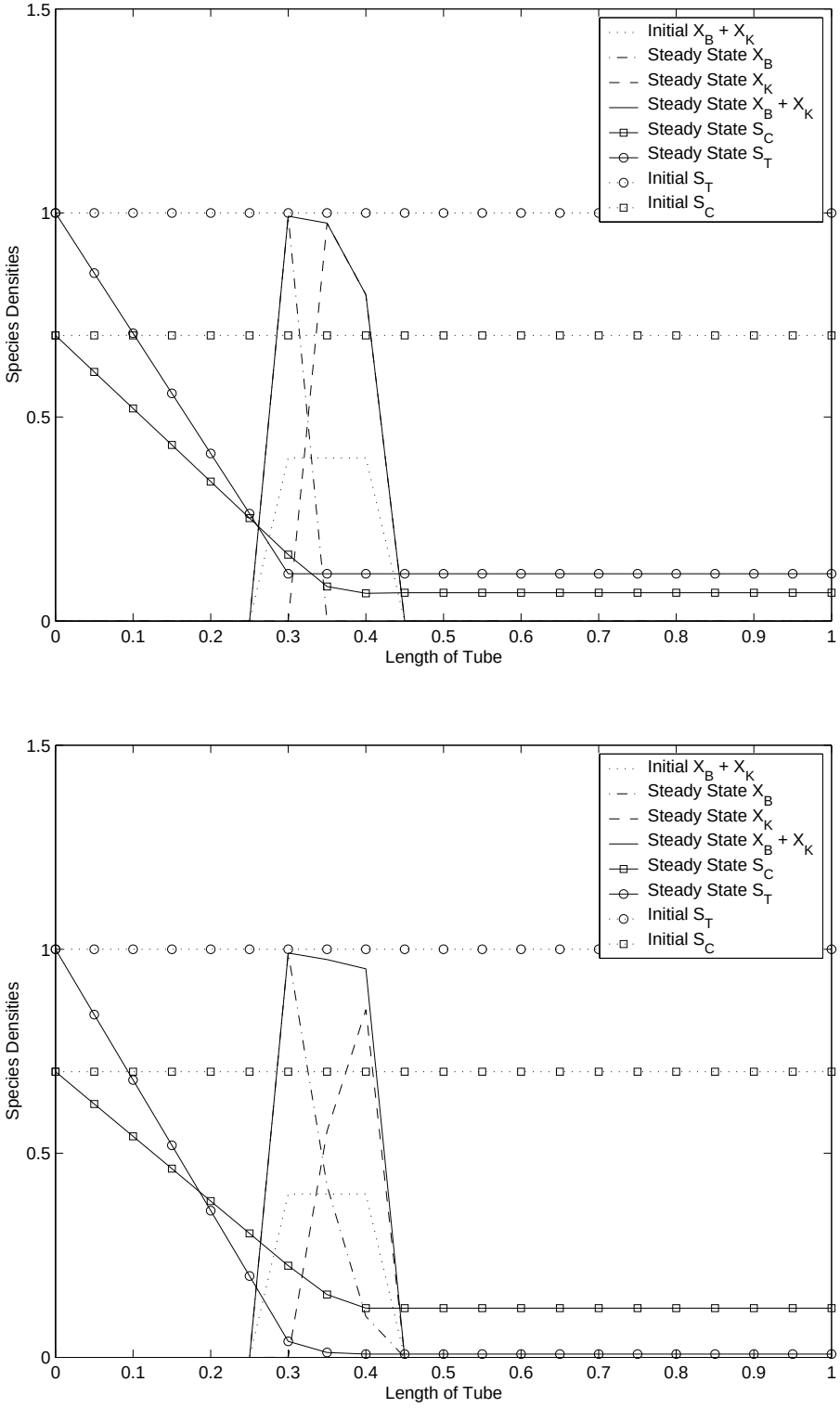

FIGURE 6. Numerical simulation results for the dual-species biobarrier model II, System (2.15), with different modified Monod kinetics, Equations (2.17) (top) and Equations (2.18) (bottom), at low nutrient supply into the system.

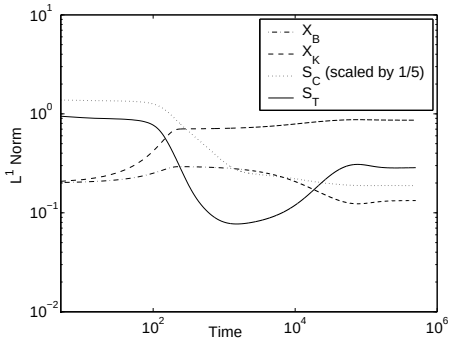

(a) System (2.15) with Equations (2.16)

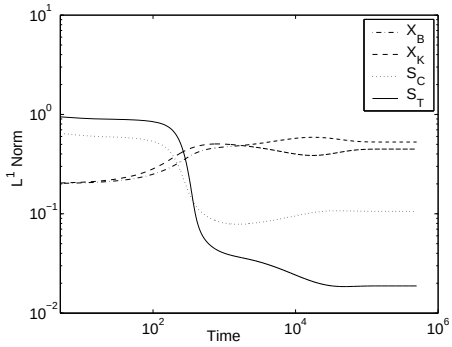

(b) System (2.15) with Equations (2.16)

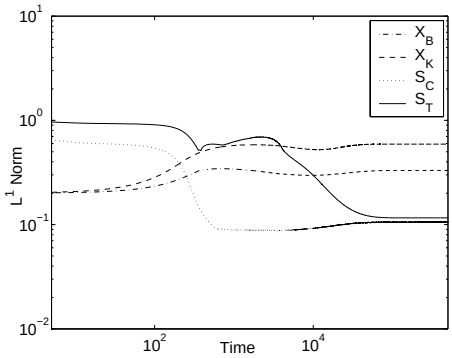

(c) System (2.15) with Equations (2.17)

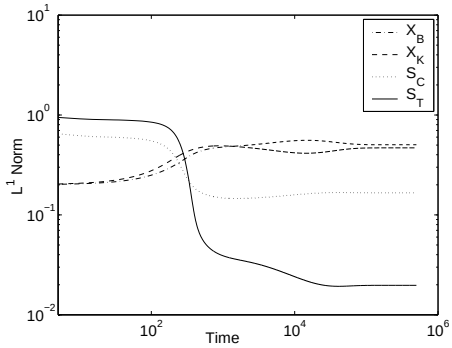

(d) System (2.15) with Equations (2.18)

FIGURE 7. Log-log scale plots of the L^1 norms of X_K, X_B, S_C, and S_T, versus time — at high nutrient (a) and at low nutrient (b), (c), and (d) supply into the system for the dual-species biobarrier model II with different Monod kinetics.